Fast Relaxation of Photo-Excited Carriers in 2-D Transition Metal Dichalcogenides

DOI:
10.1109/JSTQE.2016.2583059

Document Version
Accepted author manuscript

Fast relaxation of photo-excited carriers in 2D transition metal dichalcogenides

Mark Danovich, Igor L. Aleiner, Neil D. Drummond, Vladimir I. Fal'ko

***Abstract*—We predict a fast relaxation of photo-excited carriers in monolayer transition metal dichalcogenides (TMDCs), which is mediated by the emission of longitudinal optical (LO) and homopolar (HP) phonons. By evaluating Born effective charges for $MoS_2, MoSe_2, WS_2,$ and WSe_2, we find that, due to the polar coupling of electrons with LO phonons, and the homopolar phonons lattice deformation potential, the cooling times for hot electrons and holes from excitation energies of several hundred meV are at ps-scale.**

***Index Terms*—TMDCs, Optoelectronics, Ultrafast relaxation**

I. Introduction

MONOLAYER transition metal dichalcogenides (TMDCs) offer a unique possibility to create nm-thin optoelectronic devices [1]–[9], in particular when used in van der Waals heterostructures with other two-dimensional (2D) crystals [10]. The optoelectronic functionality of TMDCs is determined by their high-efficiency optical absorption in the visible optical range [11] as well as the fact that their monolayers are direct-band-gap 2D materials. Because of their promise for optoelectronics, it is important to understand the process of cooling (energy relaxation) of photo-excited carriers in TMDCs. In this paper we show that photo-excited carriers can emit Γ-point optical phonons at a sub-ps time scale. Such a high speed of relaxation of electrons and holes excited to energies $> 150\,\mathrm{meV}$ above the band edge arises from polar coupling to the longitudinal optical (LO) phonons, and the deformation potential induced by the out of plane homopolar (HP) phonon mode. In the theory reported in this Letter, we analyze the phonon-mediated cooling of hot electrons/holes in TMDCs, taking into account two phonon modes coupled to the intra-band intra-valley relaxation processes: the in-plane LO phonon and the out of plane HP vibrational mode [12]. Density functional theory (DFT) modeling produces electron (hole) couplings to the corner of the Brillouin zone (K-point) phonons, which are weaker by at least an order of magnitude [13]–[17]. We also note that advance DFT methods have shown that the energy difference between the Q and K valleys in the conduction band in MoS_2 and $MoSe_2$ are large enough to exclude $K \to Q$ scattering from our considerations [15], [18].

M. Danovich is with the National Graphene Institute, University of Manchester, Booth St E, Manchester M13 9PL, UK. (e-mail: mark.danovich@postgrad.manchester.ac.uk).

I. L. Aleiner is with the Physics Department, Columbia University, New York, NY 10027, USA. (e-mail: aleiner@phys.columbia.edu)

N. D. Drummond is with the Department of Physics, Lancaster University, Lancaster LA1 4YB, United Kingdom. (e-mail: n.drummond@lancaster.ac.uk).

V. I. Fal'ko is with the National Graphene Institute, University of Manchester, Booth St E, Manchester M13 9PL, UK. (e-mail: vladimir.falko@manchester.ac.uk).

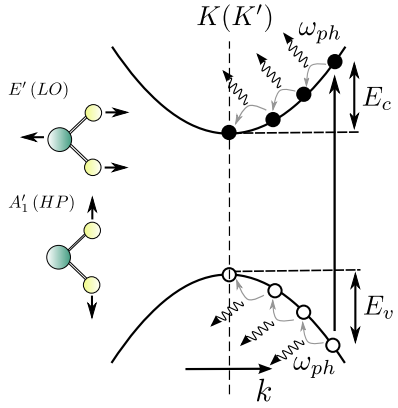

Fig. 1. Sketch of the energy relaxation of photo-excited carriers in the valence (v) and conduction (c) bands of TMDCs through phonon emission. The use of the parabolic approximation in the description of electron and hole dispersion in each valley (K or K') sets a constraint, $E \leq 0.25\,\mathrm{eV}$ on the excitation energies of the charge carriers. The insets show side view of the atomic displacements in the LO and HP modes.

II. Carrier-phonon interaction

The carrier-phonon interaction in TMDCs is given by the Hamiltonian

$$H_{e-ph} = \sum_{\substack{\vec{q},\vec{k} \\ \mu=LO,HP}} g_{\mu,\vec{q}} c^\dagger_{\vec{k}+\vec{q}} c_{\vec{k}} (a^\dagger_{\mu,-\vec{q}} + a_{\mu,\vec{q}}), \qquad (1)$$

where $c^\dagger_{\vec{k}}\,(c_{\vec{k}})$ are the creation (annihilation) operators for a charge carrier (electron or hole) in the vicinity of one of the valleys, (K or K'), near the corners of the hexagonal Brillouin zone of the 2D crystal [19], [20], with $\vec{k}$ measured from the valley center (see Fig. 1). The operators $a^\dagger_{\mu,\vec{q}}(a_{\mu,\vec{q}})$ are the phonon creation (annihilation) operators for mode $\mu =$ LO or HP with wavevector $\vec{q}$, where $|q| \ll |K|$. The two phonon modes[1] accounted for in the relaxation process are shown in Fig. 1.

The LO mode, which corresponds to the irreducible representation E' of the symmetry group D_{3h} of the crystal, couples to the charge carriers through the polarization induced by the lattice deformation, $\vec{P} = \frac{Ze}{A}\vec{u}$, where Z is the Born charge, $\vec{u}$

[1]TMDCs have 6 optical modes denoted by the irreducible representations of the point group D_{3h} (A_1', A_2'', E', E''), and 3 acoustical modes denoted by LA, TA, and ZA, where LA and TA are the in-plane longitudinal and transverse modes, and ZA is the out-of-plane mode. We neglect the transverse optical and acoustical modes due to their weak coupling at the Γ point, $q \to 0$.

TABLE I
TMDC PARAMETERS USED IN THE MODELLING OF THE PHONON EMISSION RATES.

	MoS_2	$MoSe_2$	WS_2	WSe_2
$\frac{m_c}{m_0}$ Ref. [11]	0.46	0.56	0.26	0.28
$\frac{m_v}{m_0}$ Ref. [11]	0.54	0.59	0.35	0.36
A [Å^2] Ref. [11]	8.65	9.37	8.65	9.37
$\frac{M_r}{m_p}$	38.4	59.7	47.5	85.0
$\frac{M}{m_p}$	160	254	248	342
$\hbar\omega_{LO}$ [meV] Ref. [13]	49	37	44	31
$\hbar\omega_{HP}$ [meV] Ref. [13]	51	30	52	31
D_c [eV/Å] Ref. [13]	5.8	5.2	3.1	2.3
D_v [eV/Å] Ref. [13]	4.6	4.9	2.3	3.1
Z	−1.08	−1.80	−0.47	−1.08
r_* [Å] Ref. [21]	41	52	38	45

is the relative displacement of the two sublattices in the LO vibration, A is the unit cell area, and e is the electron charge.

To estimate the Born charge we used DFT [22] to calculate the Born effective charges of the atoms in the lattice of monolayer TMDCs. The latter are defined by the response of the atomic displacements in a unit cell to a homogeneous electric field. Hence, we write

$$Z \equiv Z_{xx} = Z_{yy};\ Z_{ij} = \frac{1}{e}\frac{\partial F_j(s)}{\partial E_i}\bigg|_{\mathbf{E}=\mathbf{0}}, \qquad (2)$$

where $\mathbf{F}(s)$ is the force acting on atom s at its zero-field equilibrium position. We used the CASTEP plane-wave basis code [23], [24] to calculate the Born effective charge tensors for $MoS_2, MoSe_2, WS_2$, and WSe_2;[2] see Table I. We used the Perdew–Burke–Ernzerhof [27] (PBE) exchange–correlation functional, norm-conserving pseudopotentials, a plane-wave cutoff energy of $\sim 816\,\mathrm{eV}$, a 97×97 Monkhorst–Pack grid of $\mathbf{k}$-points, and (for the in-plane components of the Born effective charge tensors) an artificial (out-of-plane) periodicity of $\sim 16\,\text{Å}$. We verified that our results are converged with respect to these parameters. For the out-of-plane component we found a significant dependence on the artificial periodicity, which we removed by extrapolating to infinite layer separation.

The LO phonon coupling (the same for electrons and holes) is given by[3],

$$g_{LO} = \frac{i}{A}\sqrt{\frac{\hbar}{2NM_r\omega_{LO}}}\frac{2\pi Ze^2}{1+qr_*}, \qquad (3)$$

where N is the number of unit cells, M_r is the reduced mass of the two sublattices, and ω_{LO} is the LO phonon frequency.

[2]Note that Eq. (2) is evaluated using Eqs. (40) and (42) of Ref. [25]. To evaluate Eq. (42) of Ref. [25], derivatives of the Kohn–Sham orbitals with respect to the atomic positions and with respect to the wavevector are required. The latter are evaluated within the parallel-transport gauge by minimizing the functional in Eq. (70) of Ref. [26].

[3]Starting from the electrostatic interaction energy in 2D, $E = \frac{1}{2}\int \frac{d^2\vec{r}d^2\vec{r}'}{|\vec{r}-\vec{r}'|}\sigma(\vec{r})\sigma(\vec{r}') + \frac{1}{2\kappa}\int d^2\vec{r}(P_\perp^2 + P_{op}^2)$, with $\sigma(\vec{r}) = e\rho(\vec{r}) - \nabla\cdot\vec{P}_{op}(\vec{r}) - \nabla\cdot\vec{P}_\perp(\vec{r})$, where $\rho(r)$ is the 2D carrier density, $\vec{P}_{op}$ is the optical phonon induced polarization, $\vec{P}_\perp$ is the remaining in-plane polarization, and κ is the in-plane rigidity. Assuming the adiabatic approximation, we Fourier transform the integrand, and integrate out $P_\perp$, we obtain the dielectric screening $1/(1+2\pi\kappa q)$, from which we define the screening length as $r_* = 2\pi\kappa$, and the carrier-phonon coupling is obtained from the term containing $\rho_q^*\vec{P}_{op,q}$, which are the Fourier components of the electron density and the optical phonon induced polarization vector.

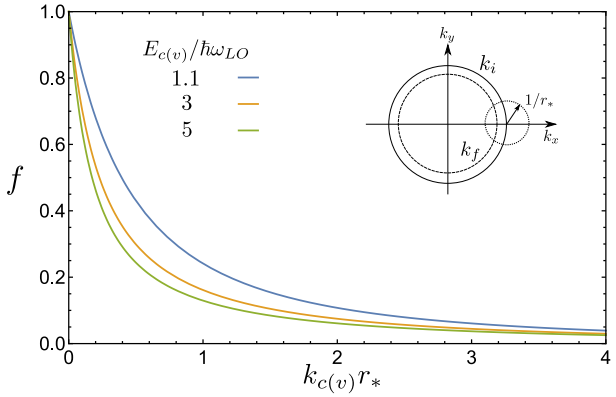

Fig. 2. The dimensionless function $f(k_{c(v)}r_*)$ in Eq. (5a) for different carrier energies, $E_{c(v)}/\hbar\omega_{LO} = 1.1, 3$ and 5. The inset sketches the kinematics for the phonon emission process in momentum space for the carrier undergoing energy relaxation with initial state wavevector k_i and final-state wavevector k_f. The circle with radius $1/r_*$ defines the region of phonon wavevectors q that give the dominant contribution to the scattering rate. As the number of available final states scales as the circumference of the iso-energy circle in momentum space, for a given r_* the asymptotic behavior of the scattering rate for high carrier energies is given by $\tau \sim 1/k_i \propto 1/\sqrt{E}$.

The dielectric screening of the electric field of LO mode deformations is described [3], [28] by the factor $1/(1+qr_*)$, where r_* is a length scale defined by $r_* = a_z(\epsilon_{||}-1)/2$, where a_z and $\epsilon_{||}$ are the z-axis lattice constant and in-plane dielectric constant of a bulk crystal of the corresponding TMDC [21], [28]. The values used for the screening lengths are taken from the DFT calculated 2D polarizabilities in Ref. [21].

The homopolar (HP) mode (which corresponds to the irreducible representation A_1' of the symmetry group D_{3h}) couples with the carriers through the lattice deformation potential[4]

$$g_{HP}^{\alpha} = \sqrt{\frac{\hbar}{2NM\omega_{HP}}}D^{\alpha}, \qquad \alpha = c \text{ or } v, \qquad (4)$$

where M is the total atomic mass within the unit cell, ω_{HP} is the HP phonon frequency, and we distinguish electrons in the conduction band (c) and holes in the valence band (v). Here we follow the definitions given in Refs. [13], [14], [18] for the coupling and, below, we use the deformation potentials for the HP phonon mode reported in Ref. [13].

III. SCATTERING RATES

The emission of both LO and HP phonons by a photo-excited electron/hole with initial momentum k_i measured from the center of the corresponding (K or K') valley, is characterized by the rate calculated using the Fermi golden rule,

$$\tau^{-1} = \frac{2\pi}{\hbar}\sum_{\vec{q},\mu}|\langle f|H_{e-ph}|i\rangle|^2\delta(E_f - E_i).$$

[4]For the LO/TO mode at the Γ-point, the pseudo-potential induced by the atomic displacements, which is a scalar function, will contain the factor $\nabla\cdot\vec{u}$. Hence, it would appear in the power-law expansion together with the wavevector $\vec{q}$ of the phonon, and will vanish at the Γ-point. For the LO phonon mode, this factor q is canceled by the $1/q$ factor coming from the 2D Fourier transform of the Coulomb potential, resulting in a finite contribution at the Γ-point in Eq. (3).

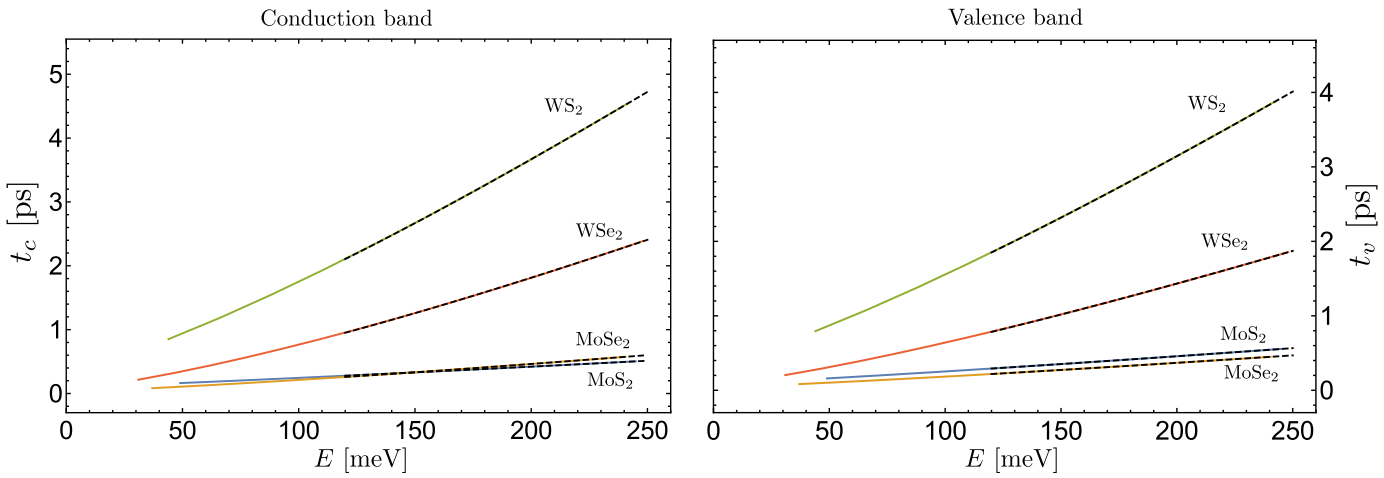

Fig. 3. Hot carrier cooling time as a function of initial conduction-band (Left) and valence-band (Right) carrier energy E for four TMDC materials. The dashed lines are asymptotic fits of the form in Eq. (6c).

This yields

$$\tau_{LO,\alpha}^{-1} = \tau_\alpha^{-1} f\left(\frac{E_\alpha}{\hbar\omega_{LO}}, k_\alpha r_*\right), \qquad \alpha = c \text{ or } v$$
$$\tau_\alpha^{-1} = \frac{2\pi^2 Z^2 E_B}{\hbar}\frac{m_\alpha}{M_r}\frac{a_B^2}{A}\frac{E_B}{\hbar\omega_{LO}};$$
$$f = \frac{1}{\pi}\frac{k_\alpha}{k_i}\int_{u_-}^{u_+}\frac{du}{(1+uk_\alpha r_*)^2\sqrt{1-[\frac{k_\alpha}{2k_i}(u+\frac{1}{u})]^2}}; \tag{5a}$$
$$u_\pm = \frac{k_i}{k_\alpha}\left(1 \pm \sqrt{1-\frac{k_\alpha^2}{k_i^2}}\right); \quad k_\alpha = \sqrt{\frac{2m_\alpha\omega_{LO}}{\hbar}};$$

$$\tau_{HP,\alpha}^{-1} = \frac{m_\alpha A D_\alpha^2}{2M\hbar^2\omega_{HP}}. \tag{5b}$$

Note that these scattering rates are valid only for carrier energies above the corresponding optical phonon energy. Furthermore, the rate of emission of the HP phonon is independent of the carrier energy, due to the constant coupling coefficient and the constant density of states for 2D carriers with parabolic dispersion. For the LO phonon mode we express the scattering rate in terms of a dimensionless integral by performing a change of variables, defining the dimensionless variable $u = q/k_{c(v)}$, where $k_{c(v)}$ is the carrier wavevector corresponding to an energy of $\hbar\omega_{LO}$, and a_B and E_B are the Bohr radius and energy. In Table II we list the values of the parameter $\tau_{c(v)}^{-1}$ for various TMDCs, and in Fig. 2 we show the shape of the function f for different carrier energies $E_{c(v)}$. The decrease of this scattering rate upon increasing r_* or excitation energy can be understood from the diagram depicting the kinematic phase space for a carrier emitting an optical phonon.

Comparing the values of $\tau_{c(v)}^{-1}$ and $\tau_{HP,c(v)}^{-1}$ in Eqs. (5a), (5b), and Table II, we see that emission of the LO phonon mode with $r_* = 0$, dominates in the relaxation over the HP phonon. The two rates become comparable for sufficiently large carrier energies or sufficiently large r_* values. Asymptotically, we have for the LO phonon, $\tau_{LO}^{-1} \sim 1/(r_*\sqrt{E})$; therefore, the boundary between the two modes is given by[5] $\frac{r_*\sqrt{mE}}{\hbar} \sim 4\pi Z^2 \frac{a_B^2 E_B^2}{A^2 D_\alpha^2}\frac{M}{M_r}\frac{\omega_{HP}}{\omega_{LO}}$, where E is the energy of the photo-excited carrier and m is its band mass.

IV. Relaxation Times

For hot carriers excited to the energy $E \gg \hbar\omega_{LO/HP}$, we write the cooling rate as

$$\frac{dE}{dt} = -\frac{\hbar\omega_{LO}}{\tau_{LO}(E)} - \frac{\hbar\omega_{HP}}{\tau_{HP}}, \tag{6a}$$

so that we can determine the relaxation time as a function of the initial carrier energy E as

$$t(E) = \int_0^E \frac{d\epsilon}{\frac{\hbar\omega_{LO}}{\tau_{LO}(\epsilon)} + \frac{\hbar\omega_{HP}}{\tau_{HP}}}. \tag{6b}$$

For hot carriers excited to the energy $E \gg \hbar\omega_{LO/HP}$, Eqs. (5a), (5b) yield $\tau_{LO}^{-1} \propto 1/\sqrt{E}$ (also see Fig. 2) and τ_{HP}^{-1} is a constant, so that we find an analytical asymptotic form for the cooling time of charge carriers from the initial energy E to the bottom of the band,

$$t(E) \approx aE - b\sqrt{E} + c. \tag{6c}$$

The fitted values of the parameters a, b and c for the conduction and valence bands relaxation times are listed in Table II and correspond to the numerically obtained [29] relaxation time curves shown in Fig. 3 for the conduction (c) and valence (v) bands.

V. Conclusion

We calculated the scattering rates and relaxation times of photo-excited carriers in TMDCs due to optical phonon emission. We obtained relaxation times of a few ps for all the materials studied, with $MoSe_2$ and MoS_2 having the shortest

[5]This parameter was derived by equating $\tau_{LO}^{-1} \sim \tau_{HP}^{-1}$, and using the asymptotic form of τ_{LO}^{-1} for large carrier energies. The corresponding values are, 13, 18, 15 and 57 for electrons and 20, 21, 27, and 31 for holes in MoS_2, $MoSe_2$, WS_2, and WSe_2, respectively.

TABLE II
VALUES OF DERIVED AND FITTED PARAMETERS IN EQS. (5) AND (6).

	MoS_2	$MoSe_2$	WS_2	WSe_2
k_c [Å^{-1}]	0.077	0.074	0.055	0.048
k_v [Å^{-1}]	0.083	0.076	0.064	0.054
τ_c^{-1} [ps^{-1}]	112	296	11	45
τ_v^{-1} [ps^{-1}]	130	312	14	58
${\tau_{HP,c}}^{-1}$[ps^{-1}]	6.8	7.7	0.69	0.54
${\tau_{HP,v}}^{-1}$[ps^{-1}]	5.0	7.2	0.5	1.3
a_c [$\frac{\text{ps}}{\text{meV}}$]	$2.3 \cdot 10^{-3}$	$3.9 \cdot 10^{-3}$	0.029	0.017
b_c [$\frac{\text{ps}}{\sqrt{\text{meV}}}$]	0.012	0.033	0.24	0.17
c_c [ps]	0.14	0.15	1.27	0.70
a_v [$\frac{\text{ps}}{\text{meV}}$]	$2.7 \cdot 10^{-3}$	$2.6 \cdot 10^{-3}$	0.023	0.012
b_v [$\frac{\text{ps}}{\sqrt{\text{meV}}}$]	0.017	0.018	0.18	0.10
c_v [ps]	0.15	0.10	1.03	0.45

sub-ps relaxation times for all carrier energies up to $0.25\,\text{eV}$, which is determined by their respective unit cell Born charges, $Z_{\text{MoSe}_2} = -1.80$ and $Z_{\text{MoS}_2} = -1.08$, and respective optical deformation potentials (Table I). For WS_2 and WSe_2, we find smaller unit cell Born charges, $Z_{\text{WS}_2} = -0.47$ and $Z_{\text{WSe}_2} = -1.08$, and smaller HP deformation potentials, resulting in longer relaxation times. However, for these two 2D materials, an additional channel of $K \rightarrow Q$ intervalley relaxation is possible, due to a smaller E^c_{KQ} splitting than in Mo-based dichalcogenides, so that the rates shown in Eq. (5) give only the lower bound for the speed of relaxation in WS_2 and WSe_2. The Introduction of a dielectric environment through a substrate or full encapsulation, will have two main effects on the calculated relaxation times. First, the electric potential induced by the LO phonon will be reduced in the long wavelength limit by the dielectric constant of the enviorment ϵ_e, therefore reducing the LO phonon coupling by a factor of ϵ_e.[6] The HP phonon mode on the other hand will not be affected in such a way, as its coupling mechanism does not involve an electric field. Second, carriers in the TMDC monolayer can emit phonons in the substrate, thus increasing the total scattering rate. The obtained fast carrier cooling rates and the subsequent formation of excitons which can radiatively recombine and emit light, can lead to high quantum efficiencies, crucial for the range of optoelectronics device applications utilizing TMDCs, including light emitters, photodetectors, and novel valleytronic devices.

ACKNOWLEDGMENT

We thank M. Calandra, T. Heinz, K. Novoselov, M. Potemski, A. Tartakovskii, and V. Zólyomi for useful discussions. This work was supported by the Simons Foundation, the ERC Synergy Grant Hetero2D and the EC-FET European Graphene Flagship.

REFERENCES

[1] D. Jariwala, V. K. Sangwan, L. J. Lauhon, T. J. Marks, and M. C. Hersam, "Emerging device applications for semiconducting two-dimensional transition metal dichalcogenides," *ACS Nano*, vol. 8, no. 2, pp. 1102–1120, 2014. [Online]. Available: http://dx.doi.org/10.1021/nn500064s

[6]For example, full encapsulation by hexagonal Boron Nitride results in [30] $\epsilon_e = \sqrt{\epsilon_\perp \epsilon_{||}} \approx 4.4$.

[2] Q. H. Wang, K. Kalantar-Zadeh, A. Kis, J. N. Coleman, and M. S. Strano, "Electronics and optoelectronics of two-dimensional transition metal dichalcogenides," *Nat. Nanotechnol.*, vol. 7, no. 11, pp. 699–712, 11 2012. [Online]. Available: http://dx.doi.org/10.1038/nnano.2012.193

[3] A. Chernikov, T. C. Berkelbach, H. M. Hill, A. Rigosi, Y. Li, O. B. Aslan, D. R. Reichman, M. S. Hybertsen, and T. F. Heinz, "Exciton binding energy and nonhydrogenic rydberg series in monolayer ws_2," *Phys. Rev. Lett.*, vol. 113, p. 076802, Aug 2014. [Online]. Available: http://link.aps.org/doi/10.1103/PhysRevLett.113.076802

[4] X. Xu, W. Yao, D. Xiao, and T. F. Heinz, "Spin and pseudospins in layered transition metal dichalcogenides," *Nat. Nanotechnol.*, vol. 10, no. 5, pp. 343–350, 05 2014. [Online]. Available: http://dx.doi.org/10.1038/nphys2942

[5] K. F. Mak, K. He, J. Shan, and T. F. Heinz, "Control of valley polarization in monolayer mos2 by optical helicity," *Nat. Nanotechnol.*, vol. 7, no. 8, pp. 494–498, 08 2012. [Online]. Available: http://dx.doi.org/10.1038/nnano.2012.96

[6] D. Xiao, G.-B. Liu, W. Feng, X. Xu, and W. Yao, "Coupled spin and valley physics in monolayers of mos_2 and other group-vi dichalcogenides," *Phys. Rev. Lett.*, vol. 108, p. 196802, May 2012. [Online]. Available: http://link.aps.org/doi/10.1103/PhysRevLett.108.196802

[7] G. Sallen, L. Bouet, X. Marie, G. Wang, C. R. Zhu, W. P. Han, Y. Lu, P. H. Tan, T. Amand, B. L. Liu, and B. Urbaszek, "Robust optical emission polarization in mos_2 monolayers through selective valley excitation," *Phys. Rev. B*, vol. 86, p. 081301, Aug 2012. [Online]. Available: http://link.aps.org/doi/10.1103/PhysRevB.86.081301

[8] T. Cao, G. Wang, W. Han, H. Ye, C. Zhu, J. Shi, Q. Niu, P. Tan, E. Wang, B. Liu, and J. Feng, "Valley-selective circular dichroism of monolayer molybdenum disulphide," *Nat. Commun.*, vol. 3, p. 887, 06 2012. [Online]. Available: http://dx.doi.org/10.1038/ncomms1882

[9] H. Zeng, J. Dai, W. Yao, D. Xiao, and X. Cui, "Valley polarization in mos2 monolayers by optical pumping," *Nat. Nanotechnol.*, vol. 7, no. 8, pp. 490–493, 08 2012. [Online]. Available: http://dx.doi.org/10.1038/nnano.2012.95

[10] A. K. Geim and I. V. Grigorieva, "Van der waals heterostructures," *Nature*, vol. 499, no. 7459, pp. 419–425, 07 2013. [Online]. Available: http://dx.doi.org/10.1038/nature12385

[11] A. Kormányos, G. Burkard, M. Gmitra, J. Fabian, V. Zólyomi, N. D. Drummond, and V. Fal'ko, "k dot p theory for two-dimensional transition metal dichalcogenide semiconductors," *2D Mater.*, vol. 2, no. 2, p. 022001, 11 2015.

[12] H. Dery and Y. Song, "Polarization analysis of excitons in monolayer and bilayer transition-metal dichalcogenides," *Phys. Rev. B*, vol. 92, p. 125431, Sep 2015. [Online]. Available: http://link.aps.org/doi/10.1103/PhysRevB.92.125431

[13] Z. Jin, X. Li, J. T. Mullen, and K. W. Kim, "Intrinsic transport properties of electrons and holes in monolayer transition-metal dichalcogenides," *Phys. Rev. B*, vol. 90, p. 045422, Jul 2014. [Online]. Available: http://link.aps.org/doi/10.1103/PhysRevB.90.045422

[14] X. Li, J. T. Mullen, Z. Jin, K. M. Borysenko, M. Buongiorno Nardelli, and K. W. Kim, "Intrinsic electrical transport properties of monolayer silicene and mos_2 from first principles," *Phys. Rev. B*, vol. 87, p. 115418, Mar 2013. [Online]. Available: http://link.aps.org/doi/10.1103/PhysRevB.87.115418

[15] L. Zeng, Z. Xin, S.-W. Chen, G. Du, J.-F. Kang, and X.-Y. Liu, "Phonon-limited electron mobility in single-layer mos2," *Chinese Physics Lettters*, vol. 31, p. 027391, 2012.

[16] M. Calandra, private communication.

[17] V. Zólyomi, unpublishd.

[18] K. Kaasbjerg, K. S. Thygesen, and K. W. Jacobsen, "Phonon-limited mobility in n-type single-layer mos_2 from first principles," *Phys. Rev. B*, vol. 85, p. 115317, Mar 2012. [Online]. Available: http://link.aps.org/doi/10.1103/PhysRevB.85.115317

[19] G.-B. Liu, D. Xiao, Y. Yao, X. Xu, and W. Yao, "Electronic structures and theoretical modelling of two-dimensional group-vib transition metal dichalcogenides," *Chem. Soc. Rev.*, vol. 44, pp. 2643–2663, 2015. [Online]. Available: http://dx.doi.org/10.1039/C4CS00301B

[20] H. Zeng and X. Cui, "An optical spectroscopic study on two-dimensional group-vi transition metal dichalcogenides," *Chem. Soc. Rev.*, vol. 44, pp. 2629–2642, 2015.

[21] T. C. Berkelbach, M. S. Hybertsen, and D. R. Reichman, "Theory of neutral and charged excitons in monolayer transition metal dichalcogenides," *Phys. Rev. B*, vol. 88, p. 045318, Jul 2013. [Online]. Available: http://link.aps.org/doi/10.1103/PhysRevB.88.045318

[22] S. Baroni, S. de Gironcoli, A. Dal Corso, and P. Giannozzi, "Phonons and related crystal properties from density-functional perturbation

theory," *Rev. Mod. Phys.*, vol. 73, pp. 515–562, Jul 2001. [Online]. Available: http://link.aps.org/doi/10.1103/RevModPhys.73.515

[23] S. J. Clark, M. D. Segall, C. J. Pickard, P. J. Hasnip, M. I. J. Probert, K. Refson, and M. C. Payne, "First principles methods using castep," *Z. Kristallogr.*, vol. 220, p. 567, 2005. [Online]. Available: http://www.degruyter.com/view/j/zkri.2005.220.issue-5-6-2005/zkri.220.5.567.65075/zkri.220.5.567.65075.xml

[24] K. Refson, P. R. Tulip, and S. J. Clark, "Variational density-functional perturbation theory for dielectrics and lattice dynamics," *Phys. Rev. B*, vol. 73, p. 155114, Apr 2006. [Online]. Available: http://link.aps.org/doi/10.1103/PhysRevB.73.155114

[25] X. Gonze and C. Lee, "Dynamical matrices, born effective charges, dielectric permittivity tensors, and interatomic force constants from density-functional perturbation theory," *Phys. Rev. B*, vol. 55, pp. 10 355–10 368, Apr 1997. [Online]. Available: http://link.aps.org/doi/10.1103/PhysRevB.55.10355

[26] X. Gonze, "First-principles responses of solids to atomic displacements and homogeneous electric fields: Implementation of a conjugate-gradient algorithm," *Phys. Rev. B*, vol. 55, pp. 10 337–10 354, Apr 1997. [Online]. Available: http://link.aps.org/doi/10.1103/PhysRevB.55.10337

[27] J. P. Perdew, K. Burke, and M. Ernzerhof, "Generalized gradient approximation made simple," *Phys. Rev. Lett.*, vol. 77, pp. 3865–3868, Oct 1996. [Online]. Available: http://link.aps.org/doi/10.1103/PhysRevLett.77.3865

[28] B. Ganchev, N. Drummond, I. Aleiner, and V. Fal'ko, "Three-particle complexes in two-dimensional semiconductors," *Phys. Rev. Lett.*, vol. 114, p. 107401, Mar 2015. [Online]. Available: http://link.aps.org/doi/10.1103/PhysRevLett.114.107401

[29] J.-Z. Zhang, A. Dyson, and B. K. Ridley, "Momentum relaxation due to polar optical phonons in algan/gan heterostructures," *Phys. Rev. B*, vol. 84, p. 155310, Oct 2011. [Online]. Available: http://link.aps.org/doi/10.1103/PhysRevB.84.155310

[30] A. Principi, M. Carrega, M. B. Lundeberg, A. Woessner, F. H. L. Koppens, G. Vignale, and M. Polini, "Plasmon losses due to electron-phonon scattering: The case of graphene encapsulated in hexagonal boron nitride," *Phys. Rev. B*, vol. 90, p. 165408, Oct 2014. [Online]. Available: http://link.aps.org/doi/10.1103/PhysRevB.90.165408

Mark Danovich received his BSc and MSc (2014) from the Hebrew University of Jerusalem, Israel. He is Currently working towards the Ph.D. degree in Physics at the National Graphene Institute, University of Manchester, UK.

Neil D. Drummond received his PhD from Cambridge University, he is currently at the Department of Physics, Lancaster University, UK.

Igor. L. Aleiner received his PhD from the University of Minnesota (1996). He worked as a Research scientist at Nippon Electric Corporation Research Institute, Princeton, New Jersey, and at the State University of New York. He is currently at the Physics Department, Columbia University, New York, USA.

Vladimir I. Fal'ko received his PhD from the Institute for Solid State Physics RAS, Russia. He worked at the Max-Planck-Institut, Stuttgart, Germany, Oxford University, and Lancaster University, UK. He is currently the research director at the National Graphene Institute, University of Manchester, UK.